3 THOMAS, H. J., FUDGE, D. L., and MORRIS, G.: 'Gunn source integrated with microstrip patch', *Microwaves & RF*, 1985, pp. 87–89
4 CHANG, K., HUMMER, K. A., and KLEIN, J. L.: 'Experiments on injection-locking of active antenna elements for active phased arrays and spatial power combiners', *IEEE Trans.*, 1989, **MTT-37**, pp. 1078–1084
5 PERKINS, T. O.: 'Active microstrip circular patch antenna', *Microwave J.*, 1987, pp. 110–117
6 CAMILLERI, N., and BAYRAKTAROGLU, B.: 'Monolithic millimeter-wave IMPATT oscillator and active antenna', *IEEE Trans.*, 1988, **MTT-36**, pp. 1670–1676
7 CHANG, K., HUMMER, K. A., and GOPALAKRISHNAN, G. K.: 'Active radiating element using FET source integrated with microstrip patch antenna', *IEEE Trans.*, 1988, **MTT-31**, pp. 91–92
8 YORK, R. A., MARTINEZ, R. M., and COMPTON, R. C.: 'Active patch antenna element for array applications', *Electron. Lett.*, 1990, **26**, pp. 494–495
9 WANG, N., and SCHWARZ, S. E.: 'Monolithically integrated Gunn oscillator at 35 GHz', *Electron. Lett.*, 1984, **20**, pp. 603–604

NEW CLASS OF FIBRE LASER BASED ON LEAD-GERMANATE GLASS

J. R. Lincoln, C. J. Mackechnie, J. Wang, W. S. Brocklesby, R. S. Deol, A. Pearson, D. C. Hanna and D. N. Payne

Indexing terms: Glass, Optical fibres, Lasers

The first fibre laser based on rare-earth doped lead-germanate glass is reported. The thulium-doped fibre had a background loss of 2 dBm^{-1} and a maximum phonon energy of ~920 cm^{-1}. Lasing was achieved on the Tm^{3+} $^3H_4$–$^3H_6$ transition at 1·905 μm with a 3·6 mW threshold, when diode-pumped at 790 nm. A quantum efficiency of 30% was obtained.

We present a new class of rare-earth doped glass fibre which has been selected to have a maximum phonon energy of ~920 cm^{-1}, a value intermediate between the maximum phonon energies of fluoride and silica-based glasses. Because of the high maximum phonon energy in silica glasses (~1150 cm^{-1}) [1] in many rare-earth doped silica glass fibre lasers the threshold for laser operation is limited by competition between multiphonon emission and radiative emission from the upper laser level. On the other hand, multiphonon emission is often essential in the pumping process because it provides the preferred channel for the decay from the pump level to the laser level. In these cases too low a phonon energy can result in a low pumping efficiency. An example of this effect is provided by the $^3H_4$–$^3H_6$ (~1·9 μm) laser transition in Tm^{3+} (see Fig. 1). In ZBLAN, with its maximum phonon energy of 590 cm^{-1} [2], the $^3H_4$–$^3H_6$ transition has a high radiative quantum efficiency, but is limited by a low pump efficiency [3] to the $^3H_4$ level when diode-pumped via the $^3F_4$ level [4, 5]. By contrast, in silica the $^3H_4$ level has a low radiative efficiency but a high pump efficiency [6]. Thus for the Tm^{3+} 1·9 μm laser, optimum laser performance would be achieved in a host with phonon energies low enough to ensure that the $^3H_4$ level decays purely radiatively, but high enough to ensure a high, phonon-mediated, transfer rate on the $^3F_4$–$^3H_5$ transition. Inspection of the equation for multiphonon decay in solids given by Layne *et al.* [7] indicates the optimum phonon energy required is ~900 cm^{-1}. By using a modified lead germanate glass with a maximum phonon energy of ~920 cm^{-1}, we can achieve the desired optimisation of the phonon energy. We show that in fibre form this results in a low-threshold laser with good slope efficiency. Furthermore lead-germanate fibre has the benefits of sufficiently low loss, high mechanical strength and a simple method of manufacture.

The lead germanate fibre was fabricated using the rod and tube technique [8]. The core glass was a proprietary lead-germanate melt with composition GeO_2–PbO–BaO–ZnO–K_2O (abbreviated to GPBZK) and incorporating 0·5 wt% Tm_2O_3, equivalent to 8×10^{21} ion cm^{-3}. The cladding was Schott SF56 glass. The experimental and theoretical considerations that lead to this core glass composition and choice of cladding glass will be reported elsewhere. Fibre was pulled

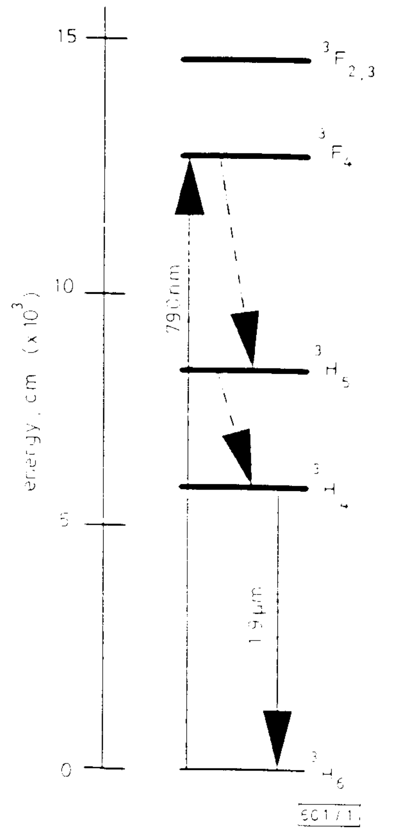

Fig. 1 *Energy level diagram of Tm^{3+} in lead-germanate glass*

Line positions were taken from bulk absorption spectra, and energy level assignment follows zero spin-orbit coupling convention

Excitation and lasing scheme for Tm^{3+} 1·9 μm laser is shown

——— radiative processes

- - - - nonradiative, phonon emission, processes

with 7 μm core diameter and a total length in excess of 50 m. The fibre had good optical properties with a high quality homogeneous core-cladding interface. Because of the high dopant concentration and the high total absorption cross-section, the absorption at the peak of the $^3F_4$ pump band was > 140 dBm^{-1}, and this allows lasers of only a few centimetres in length to be constructed. The high value for the absorption was due to both the high dopant concentration and the high absorption cross-section. The background fibre loss was 2 dBm^{-1} and probably represents the background loss the bulk glass used in the fibre core, which was limited by the purity of the starting materials. The mechanical strength of the GPBZK fibres was also good, with a bending radius of 5 mm possible in uncoated glass fibre, which is comparable with that obtainable in bare silica fibres.

The maximum phonon energy for the GPBZK core glass, as determined from the Raman spectrum of the glass, is given in Table 1, together with the measured $^3F_4$ and $^3H_4$ lifetimes for Tm^{3+} at 0·5 wt% in bulk glass. Equivalent figures are also given for ZBLAN and alumino-silicate fibre. Table 1 also gives the refractive indices of the various glasses. At 1·812 μm the refractive index of the GPBZK is substantially higher than for either silicates or fluorozirconates. Such a high refractive index yields two advantages, namely the possibility of producing very high numerical aperture fibres, further lowering the lasing threshold and increasing gain efficiency. Secondly a high refractive index yields an increase in the radiative probability and cross-section for a transition through the refractive index term in the Einstein coefficients [9].

Characterisation of the lasing properties of Tm^{3+} : GPBZK fibre was carried out using Ti : sapphire or GaAs diode lasers as pump sources. In both cases laser cavities were constructed by butting dielectric mirrors to the cleaved fibre ends and launching the pump light through one mirror.

Table 1

	Alumino-silicate	ZBLAN	GPBZK
Maximum phonon energy (cm^{-1})	1150 [1]	590 [2]	920
$^3F_4$ lifetime measured (μs)	20 [10]	1100 [3]	250
$^3H_4$ lifetime measured (μs)	500 [6]	6400 [3]	3000
Refractive index	~1·5	1·52 [11]	1·812

Lasing was achieved with only 3 cm of 7 μm core fibre pumped at 790 nm with a GaAs diode and using mirrors with 100 and 98% reflectivities from 1·8 to 2·2 μm. The laser threshold was 9 mW incident on the launch objective and the lasing wavelength was 1·905 μm. This incident power is equivalent to 3·6 mW launched, assuming a combined launch efficiency and objective transmission of 40%. With an initial fibre length of only 3 cm it was not possible to perform a fibre cutback to more accurately assess the launch efficiency. This low threshold, for a nonoptimised system, is already superior to the best thresholds achieved for Tm^{3+} doped alumino-silicate fibre, reported threshold 4·4 mW [6], and Tm^{3+} doped ZBLAN, reported threshold 50 mW [5, 4], and reflects the achievement of our aim of a low threshold fibre laser in the 2 μm region. The short length of this diode-pumped device also shows considerable promise for practical devices.

To make an initial assessment of the slope efficiency achievable from this fibre a further laser cavity was constructed with 27·3 cm of 7 μm core fibre using Ti : sapphire pumping at 794 nm. A 100% reflecting input mirror was used with lasing achieved with just Fresnel reflection feedback from the bare fibre end. The high refractive index of the GPBZK core provides a Fresnel reflection from the fibre end of ~10%, giving approximately 90% output coupling. Lasing was at a wavelength of 1·88 μm with a threshold of 43 mW of launched pump power. Slope efficiency of output power against launched pump power was measured to be 13%, equivalent to 30% quantum efficiency. This quantum efficiency can be compared to a maximum pump quantum efficiency available for this system of ~60%, an upper estimate calculated as the ratio of nonradiative to radiative emission probabilities from the 795 nm pumped $^3F_4$ level. Further improvement in the observed quantum efficiency should be achieved by optimising the fibre length. However, even without optimisation this GPBZK system, with an achieved slope efficiency of 13%, compares well to the Tm : alumina-silica system, where 17% was achieved in the optimised diode pumped system [6] and where the pump efficiency is ~100%. This 13% slope efficiency is also considerably superior to that achieved in Tm^{3+} : ZBLAN where 5·3% has been reported [5], improving to 8·3% with simultaneous lasing at 2·3 μm [3].

In conclusion, we have demonstrated that it is possible to fabricate a low-loss, high strength, intermediate phonon energy optical glass fibre doped with a rare earth. Furthermore, as anticipated from the phonon energy of the glass, we have shown that Tm^{3+} : GPBZK fibre lases in the 2 μm region with thresholds lower than silica-based fibres. The relatively high rare-earth concentration incorporated into this fibre and the high emission cross-section has resulted in very short fibre lengths for the lasers, a convenient feature for many applications such as Q switching. The combination of all these properties, together with the high mechanical strength and excellent optical properties yield a fibre which appears ideal for commercial applications.

1st April 1992

J. R. Lincoln and W. S. Brocklesby (*Department of Physics, University of Southampton, Southampton SO9 5NH, United Kingdom*)

C. J. Mackechnie, J. Wang, R. S. Deol, D. C. Hanna and D. N. Payne (*Optoelectronics Research Centre, University of Southampton, Southampton SO9 5NH, United Kingdom*)

References

1 MATSON, D. W., SHARMA, S. K., and PHILPOTTS, J. A.: 'The structure of high-silica alkali-silicate glasses: a Raman spectroscopic investigation', *J. Non-Crystalline Solids*, 1983, **58**, pp. 323–352

2 BENDOW, B., BANERJEE, P. K., DREXHAGE, M. G., GOLTMAN, J., MITRA, S. S., and MOYNIHAN, C. T.: 'Comparative study of vibrational characteristics of fluorozirconate and fluorohafnate glasses', *J. Am. Ceram. Soc.*, 1982, **65**, (1), pp. C8–C9

3 CARTER, J. N., SMART, R. G., TROPPER, A. C., and HANNA, D. C.: 'Thulium doped fluorozirconate fibre lasers', *J. Non-Crystalline Solids*, 1992, **140**, pp. 10–15

4 ALLAIN, J. Y., MONERIE, M., and POIGNANT, H.: 'Tunable CW lasing around 0·82, 1·48, 1·88 and 2·35 μm in thulium-doped fluorozirconate fibre', *Electron. Lett.*, 1989, **25**, pp. 1660–1662

5 SMART, R. G., CARTER, J. N., TROPPER, A. C., and HANNA, D. C.: 'Continuous-wave oscillation of Tm^{3+}-doped fluorozirconate fibre lasers around 1·47 μm, 1·9 μm and 2·3 μm when pumped at 790 nm', *Opt. Comm.*, 1991, **82**, pp. 563–570

6 BARNES, W. L., and TOWNSEND, J. E.: 'Highly tunable and efficient diode pumped operation of Tm^{3+} doped fibre lasers', *Electron. Lett.*, 1990, **26**, (11), pp. 746–747

7 LAYNE, C. B., LOWDERMILK, W. H., and WEBER, M. J.: 'Multiphonon relaxation of rare-earth ions in oxide glasses', *Phys. Rev. B.*, 1977, **16**, (1), pp. 10–20

8 TAYLOR, E. R., TAYLOR, D. T., LI, L., TACHIBANA, M., TOWNSEND, J. E., WANG, J., WELLS, P. J., REEKIE, L., MORKEL, P. R., and PAYNE, D. N.: 'Application-specific optical fibres manufactured from multicomponent glasses'. Optical Fiber Materials and Processing Materials Research Conf., Symp. Proc., Boston, 1989, pp. 321–327

9 IMBUSCH, G. F., and KOPELMEN, R.: *In* YEN, W. M., and SELZER, P. M.: 'Laser excitation fluorescence spectroscopy in glass' (Springer Verlag, New York, 1981), p. 3

10 LINCOLN, J. R., BROCKLESBY, W. S., CUSSO, F., TOWNSEND, J. E., TROPPER, A. C., and PEARSON, A.: 'Time resolved and site selective spectroscopy of thulium doped into germano- and alumino-silicate optical fibres and preforms', *J. Luminescence*, 1991, **50**, pp. 297–308

11 FRANCE, P. W., CARTER, S. F., MOORE, M. W., and DAY, C. R.: 'Progress in fluoride fibres for optical communications', *Br. Telecom. Technol. J.*, 1987, **5**, (2), pp. 28–43

STABILITY REGIONS OF RECURRENT TYPE NEURAL NETWORKS

K. Ciliz and A. Harova

Indexing terms: Stability, Neural networks

The stability regions of the stable equilibria of the Hopfield type recurrent neural networks are investigated. The dimensions of these regions directly determine how much partial information is needed for an imperfect pattern to approach a desired pattern. Therefore estimation of such regions is instrumental in the analysis of analogue recurrent neural networks.

Introduction: Artificial neural networks (ANNs) have emerged as viable alternatives to conventional computational systems. Specifically, recurrent type neural networks which were introduced by Hopfield [1] were shown to be used for various optimisation problems [2] and also as effective associative memory elements [1].

In the analysis of feedback neural networks, estimation of the stability regions of equilibrium points is important, because the success of recalling a desired pattern vector from partial information is directly related to the stability boundaries of the corresponding equilibrium point. The larger the domain of attraction of an equilibrium point, the better the recalling performance for the pattern vector associated with that equilibrium point. This means that the pattern vector can be recalled with less partial information. In a recent work by Michel *et al.* [3], the dynamics of a feedback type neural network is analysed in the framework of interconnected systems and a method for the estimated of the stability region is also proposed. In this Letter a constructive and iterative procedure is used to estimate the stability region of an equi-